

## Influence of the virtual bound state on the low-field Hall coefficient. II. Dilute alloys of Sc, Ti, V, Co, and Ni in Al

C. Papastaikoudis and D. Papadimitropoulos

*Nuclear Research Center "Dimocritos," Aghia Paraskevi, Athens, Attiki, Greece*

(Received 20 April 1981)

Very accurate measurements have been made of the low-field Hall coefficient  $R_H^0$  of rapidly quenched Al-Sc, Al-Ti, Al-V, Al-Co, and Al-Ni alloys in a magnetic field up to about 40 kG and at 4.2 K. With the exception of the Al-Sc alloy the values of  $R_H^0$  show a systematic dependence on the valence of the 3d impurities. The results are discussed in the light of the Friedel-Anderson model of localized virtual states in metals.

### I. INTRODUCTION

In the low-field region there is  $\omega_h \tau_h \ll 1$  on all points  $\vec{k}$  of the Fermi surface (FS), and the local values  $\omega_h \tau_h$  are the mean angles of rotation of the electrons between two scattering processes. The low-field Hall coefficient  $R_H^0$  is sensitive to local scattering on the Fermi surface<sup>1</sup> and for a cubic metal such as aluminum is given by the generalized formula<sup>2,3</sup>

$$R_H^0 = - \frac{12\pi^3}{ec} \frac{\int_{\text{FS}} \langle 1/\kappa \rangle \tau^2(\vec{k}) v^2(\vec{k}) dS}{\left( \int_{\text{FS}} \tau(\vec{k}) v(\vec{k}) dS \right)^2} \quad (1)$$

$\langle 1/\kappa \rangle = \frac{1}{2} (1/\kappa_1) + (1/\kappa_2)$  is the local mean curvature at a point  $\vec{k}$  on the Fermi surface,  $\kappa_1$  and  $\kappa_2$  are the local principal radii of curvature,  $\tau(\vec{k})$  is the relaxation time, and  $v(\vec{k})$  the electron velocity, with the integration extended over the Fermi surface. The integral in the denominator is proportional to  $\rho_0^{-2}$ , where  $\rho_0$  is the electrical resistivity.

$R_H^0$  will be dominated by the values of  $\tau(\vec{k})$  of those parts of the Fermi surface which have high mean curvature  $\langle 1/\kappa \rangle$ . In aluminum these regions are near the zone boundaries.

Equation (1) shows that the low-field Hall coefficient  $R_H^0$  is a normalized quantity, i.e., independent of the concentration of the same type defects.  $R_H^0$  in general is a definite function of the "effective" magnetic field  $B/\rho_0$ , if (i) the Fermi surface remains the same in a change of the defect concentration and (ii) the scattering probability is proportional to the defect concentration and independent of the magnetic field (Kohler's rule).

The present investigation on the low-field Hall coefficient  $R_H^0$  of aluminum containing Sc, Ti, V, Co, and Ni is a continuation of a previous work on Al-Cr, Al-Mn, and Al-Fe (Ref. 4, hereafter referred to as I). In I it was maintained that the existence of the 3d virtual bound states and their position relative to Fermi level is the cause for the distinct systematic dependence of

the low-field Hall coefficient  $R_H^0$  on the valence of the impurity.

In I it was assumed that if the virtual bound state (VBS) model proposed there is correct, then the  $R_H^0$  values of the rest of the Al-3d alloys (Al-Sc, Al-Ti, Al-V, Al-Co, and Al-Ni) should lie on a parabolic curve, with the lowest value at Cr. The purpose of the present investigation is to show that the assumption of the VBS model is correct, and explains the systematic dependence of  $R_H^0$  on the valence.

### II. EXPERIMENTAL PROCEDURE

The very dilute alloys of Al-Sc, Al-Ti, Al-V, Al-Co, and Al-Ni are produced from high-purity aluminum (99.999%) by the Institut für Festkörperforschung der Kernforschungsanlage, Jülich, Germany. The alloys were prepared by HF-levitation melting under an ultrapure He gas at subatmospheric pressure and then rolled into polycrystalline foils of about 200  $\mu\text{m}$  thickness. The sample shapes, which were stamped out from these foils with a special steel press tool, were rectangular (20  $\times$  2 mm<sup>2</sup>) with two similar extensions for the magnetoresistance contacts and two other central extensions for the Hall contacts. The thickness of the specimens was determined with an optical microscope with an accuracy of 0.5–1% and by measuring their resistance at room temperature. The difference between these two methods amounts to about 1%.

After cleaning in acetone and in boiling distilled water, the samples underwent the Boato *et al.*<sup>5</sup> treatment in order to obtain homogeneous solid solutions whenever thermodynamically possible; namely, the specimens were annealed in air for 24 h at 640 °C—a temperature just below the nearest eutectic temperature. The samples were then quenched very rapidly in iced water and thereafter kept at room temperature. The effectiveness of the solution process was monitored by residual resistivity measurements. The nominal concen-

trations were obtained by weight analysis.

The Hall voltage measurements were carried out in a conventional stainless-steel helium cryostat, which contained a superconducting solenoid. This cryocoil could produce a magnetic field up to 40 kG. All measurements were performed at 4.2 K in order to eliminate the effects of electron-phonon scattering. Further experimental details were described previously.<sup>6</sup>

### III. EXPERIMENTAL RESULTS

We discuss the following.

(a) The residual resistivities  $\rho_0(4.2\text{ K})$  of the currently investigated Al-3d transition-metal systems are collected in Table I in comparison with the previous measurements<sup>7-13</sup>. The values of the residual resistivity per atomic percent  $\rho_0/c$  or the residual resistivity ratios [RRR =  $R_{4,2}/(R_{300} - R_{4,2})$ ] per atomic percent of the present alloys are either in good agreement with previous measurements or higher, except for the case of Al-21.1 ppm Co, where three different  $\rho_0/c$  values are obtained. This means that in the Al-21.1 ppm Co alloy three different solid solubilities appeared and the cause is probably

the different quenching rates of this alloy.

(b) Figures 1, 2, 3, and 4 show the Hall coefficient  $R_H$  of the Al-Sc, Al-Ti, Al-V, Al-Co, and Al-Ni alloys in Kohler diagrams, i.e.,  $R_H$  is plotted as a function of the effective magnetic field  $B/\rho_0$ , where  $\rho_0$  is the residual resistivity of the samples at zero magnetic field. The figures show that the high-field-region Hall coefficient of the samples and especially of the Al-Co alloys seem to saturate at  $10.29 \times 10^{-5} \text{ cm}^3/\text{A s}$ , which is in good agreement with the theoretical value  $R_{00} = 10.24 \times 10^{-5} \text{ cm}^3/\text{A s}$ . Another feature of the  $R_H$  measurements on the Al-Co alloys is that  $R_H$  is independent of the various defect structures, which are formed during the quenching process. The low-field coefficients  $R_H^0$  of the alloys are practically independent of the impurity concentrations, constant, and exhibit large negative values. The observed small deviations, particularly in  $R_H^0$ , may be attributed to the errors in the determination of the thickness of the specimens.

Table I shows also the mean values of the low-field Hall coefficients  $R_H^0$  at a constant  $B/\rho_0$ . The low-field Hall coefficients  $R_H^0$  of the currently investigated alloys taken at a constant  $B/\rho_0$  value,

TABLE I. Concentration  $c$ ,  $\rho_0/c$ , RRR/ $c$ , and  $R_H^0$

| Alloys | $c$ (ppm)  | $\rho_0/c$ ( $\mu\Omega \text{ cm/at. \%}$ ) | RRR/ $c$ (at. $\%^{-1}$ ) | $R_H^0(10^{-5} \text{ cm}^3/\text{A s})$ | Authors                              |
|--------|------------|--|---------------------------|--|--------------------------------------|
| Al-Sc  | 10.24      | 6.68-8.20                                    | 2.5-3.0                   | -2.75                                    | This work                            |
|        | 21.1       | 5.32-5.75                                    | 1.97-2.15                 | -2.75                                    | This work                            |
|        | 500-32800  | 3.5  | 1.4                       |  | Ocko <i>et al.</i> <sup>11</sup>     |
|        | 140-2000   | 3.4  |                           |  | Fujikawa <i>et al.</i> <sup>12</sup> |
|        | ?          | 5.0  |                           |  | Fickett <sup>13</sup>                |
| Al-Ti  | 10.3       | 10.3   | 3.8                       | -2.35                                    | This work                            |
|        | 21.1       | 5.7  | 2.2                       | -2.35                                    | This work                            |
|        | 500-5000   | 5.2-5.9                                      |                           |  | Babic <i>et al.</i> <sup>7,8</sup>   |
|        | 10-250     |  | 2.4                       |  | Aoki <i>et al.</i> <sup>9</sup>      |
| Al-V   | 10.3       | 11.3   | 4.3                       | -2.5                                     | This work                            |
|        | 21.1       | 8.3  | 3.2                       | -2.5                                     | This work                            |
|        | 50-8500    | 11-7.5                                       |                           |  | Babic <i>et al.</i> <sup>7,8</sup>   |
|        | 10-400     |  | 2.9                       |  | Aoki <i>et al.</i> <sup>9</sup>      |
| Al-Co  | 10.3       | 5.4  | 2.03                      | -1.7                                     | This work                            |
|        | 21.1       | 2.2  | 0.83                      | -1.7                                     | This work                            |
|        | 21.1       | 3.0  | 1.14                      | -1.7                                     | This work                            |
|        | 21.1       | 7.5  | 2.80                      | -1.7                                     | This work                            |
|        | until 3000 | 5.0  |                           |  | Babic <i>et al.</i> <sup>8</sup>     |
| Al-Ni  | 10.3       | 7.4  | 2.8                       | -1.1                                     | This work                            |
|        | 21.1       | 4.9  | 1.9                       | -1.1                                     | This work                            |
|        | until 3000 | 2.2  |                           |  | Babic <i>et al.</i> <sup>7</sup>     |
|        | 10-300     |  | 1.2                       |  | Aoki <i>et al.</i> <sup>9</sup>      |
|        | 500        | 3.8  |                           |  | Krsnik <i>et al.</i> <sup>10</sup>   |

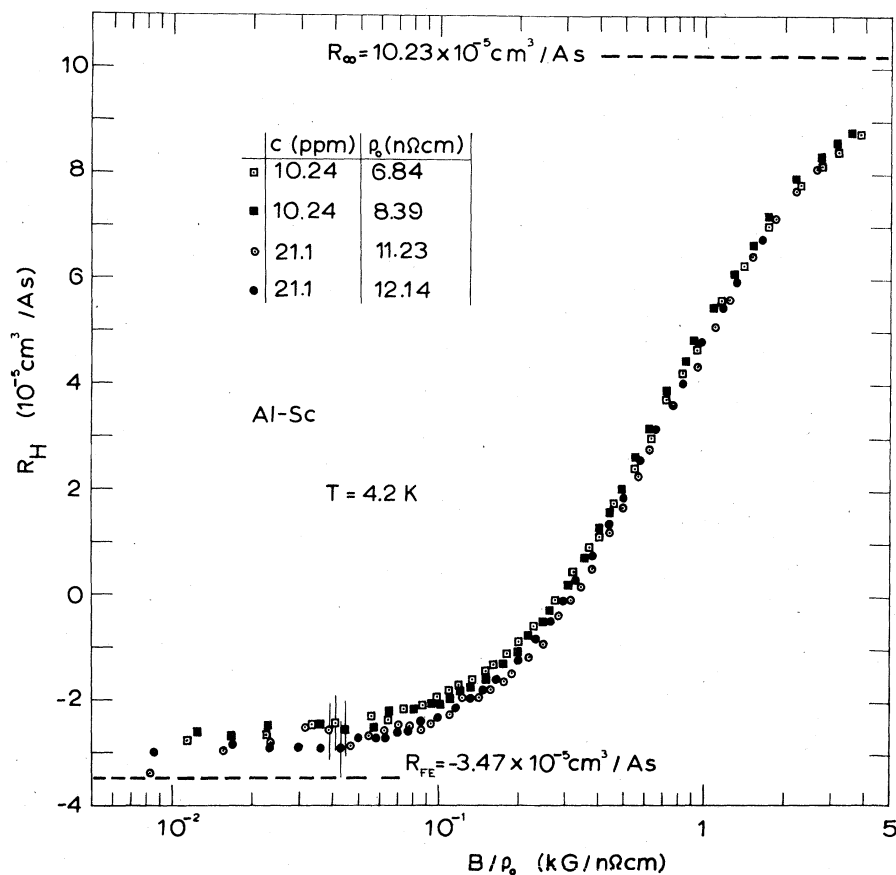


FIG. 1. Kohler plot of the Hall coefficient  $R_H$  as a function of  $B/\rho_0$  for the Al-Sc alloys.

together with the values of the earlier measurements for Al-Cr (Refs. 4 and 14), Al-Mn (Refs. 4 and 14), Al-Fe (Ref. 4), and Al-Cu (Ref. 6), are plotted in Fig. 5 as a function of the atomic number of the  $3d$  elements. It is seen from Fig. 5 that  $R_H^0$  shows a distinct systematic dependence on the impurities, similar to that found in the residual resistivity, the thermopower, and the superconducting transition temperature.  $R_H^0$  is always negative and its dependence on the atomic  $d$ -occupation number shows a parabolic form with the lowest value at chromium. The Al-Sc alloys, which exhibit a lower  $R_H^0$  value than expected, constitute an exception to the parabolic dependence. The parabolic dependence of  $R_H^0$  on the valence indicates that resonance scattering is playing an important role in determining of  $R_H^0$ .

#### IV. DISCUSSION

According to the Friedel-Anderson model<sup>15,16</sup> the virtual bound states are originated by the  $d$  states of the transitional impurity atoms, when

these are dissolved in a metal such as aluminum. The atomic  $d$  states are characterized by the position  $\epsilon_d$  measured relative to the Fermi level of the metal and by the half-width  $\Gamma$ . The width parameter  $\Gamma$  is related to the average  $s$ - $d$  admixture matrix element  $\langle V_{sd} \rangle$  and the electronic density of states  $N_s(0)$  of the host conduction band at the Fermi level by

$$\Gamma = \pi N_s(0) |\langle V_{sd} \rangle|^2. \quad (2)$$

In the Hartree-Fock approximation the density of  $d$  states per spin at the Fermi level may be written

$$N_d(\epsilon) = \frac{2l+1}{\pi} \frac{\Gamma}{(\epsilon - \epsilon_d)^2 + \Gamma^2}, \quad (3)$$

where  $(2l+1)$  arises from the orbital degeneracy of the  $d$  state in the absence of crystal-field effects.

For a nonmagnetic transition-element impurity in a normal host, when a conduction electron approaches the impurity site with an energy near

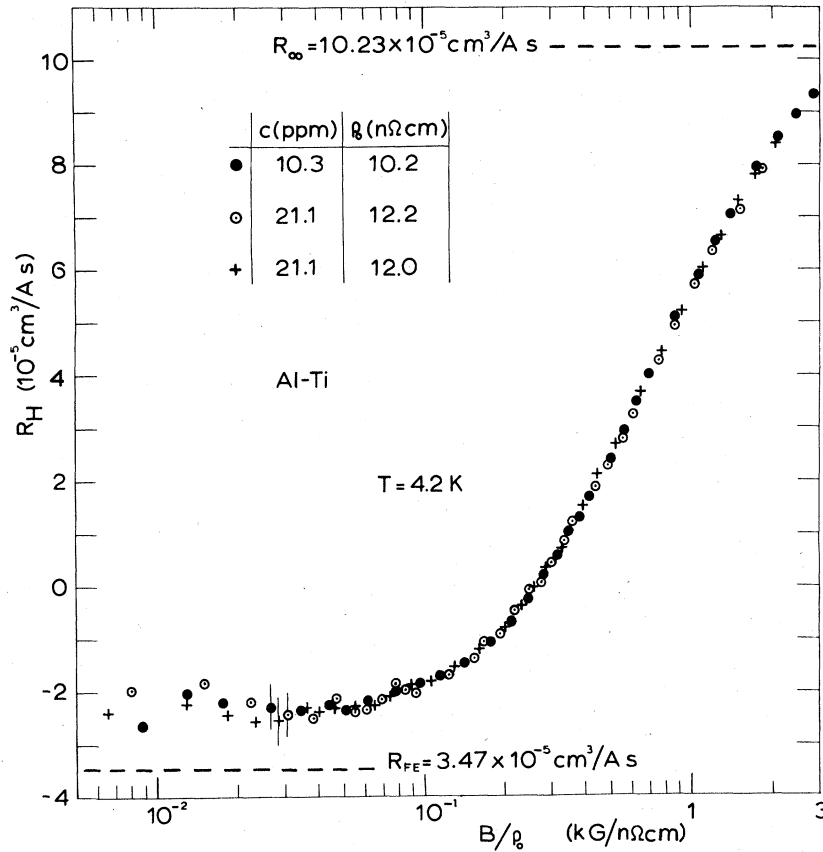


FIG. 2. Kohler diagram of the Hall coefficient  $R_H$  as a function of  $B/\rho_0$  for the Al-Ti alloys.

$\epsilon_d$ , it will be captured and resonantly scattered. The particular phase shift corresponding to the angular momentum  $l$  of the resonant state will be large. For incident energies of the conduction electrons far from the resonant energies, the phase shifts are small and the results are those of the Coulomb potential scattering. In the case of the transition atom impurity  $l=2$  the phase shifts can be written as<sup>17</sup>

$$\eta_l = \begin{cases} \eta_l^0, & l \neq 2 \\ \eta_2^0 + \cot^{-1}(\epsilon_d - \epsilon) / \Gamma = \eta_2^0 + \eta_2^{res}, & l = 2 \end{cases} \quad (4)$$

where  $\eta_l^0$  are the nonresonant phase shifts due to Coulomb scattering and  $\eta_2^{res}$  are the  $d$ -state phase shifts.

As a result of the above scattering process, charge accumulates in the vicinity of the impurity and locally screens the impurity potential. The total screening charge is given by the Friedel sum rule<sup>15</sup>

$$Z_{tot} = \frac{1}{\pi} \sum_l (2l+1) \eta_l^0(\epsilon_F) + \frac{5}{\pi} \cot^{-1} \left( \frac{\epsilon_d - \epsilon_F}{\Gamma} \right) = Z_{nr} + Z_{res}, \quad (5)$$

where  $Z_{nr}$  is the nonresonant part related to the phase shifts  $\eta_l^0$  and is given by the relative valence between the impurity and the host atoms, i.e.,  $Z_{nr} = Z_i - Z_h$ , while  $Z_{res}$  is the resonant part and is equal to the mean occupation number  $\langle N \rangle$  of  $d$  electrons localized on the impurity atom.

In the quasifree approximation, the total relaxation time  $\tau_{tot}$  can be expressed by the method of partial waves as

$$\tau_{tot}^{-1} = \tau_{nr}^{-1} + \tau_{res}^{-1} = \frac{4c}{\pi \hbar N(\epsilon_F)} \sum_{l>0} (2l+1) \sin^2 \eta_l, \quad (6)$$

where  $c$  is the impurity concentration and  $N(\epsilon_F)$  is the density of states at Fermi level.

According to Klein and Heeger<sup>17</sup> it is assumed for real metals that the nonresonant phase shifts are small relative to this arising from the resonant term, and thus the total screened charge and the total relaxation time can be reduced to

$$Z_{tot} \cong Z_{res} = \frac{5}{\pi} \cot^{-1} \left( \frac{\epsilon_d - \epsilon_F}{\Gamma} \right) \quad (7)$$

and

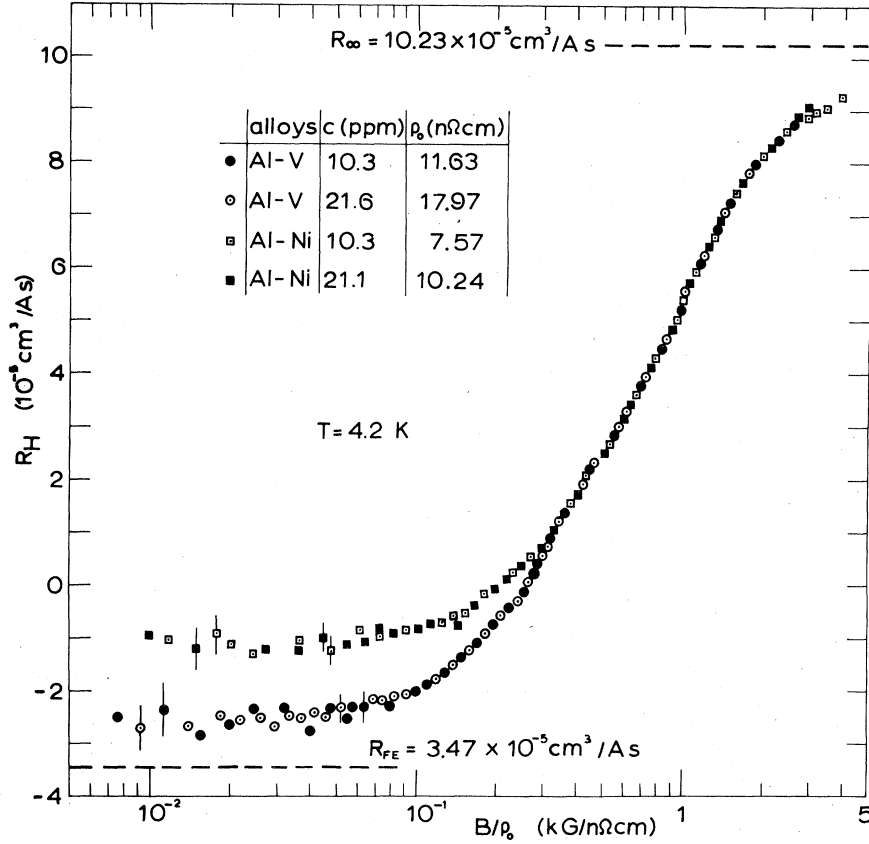


FIG. 3. Kohler plot of the Hall coefficient  $R_H$  as a function of  $B/\rho_0$  for the Al-V and Al-Ni alloys.

$$\tau_{\text{tot}}^{-1} \cong \tau_{\text{res}}^{-1} = \frac{20c}{\pi \hbar N(\epsilon_F)} \sin^2 \eta_2^{\text{res}}, \quad (8)$$

respectively.

Thus the expression (1) for the low-field Hall coefficient  $R_H^0$  can be written as

$$R_H = -\frac{12\pi^3}{ec} \frac{\int_{\text{FS}} \langle 1/\kappa \rangle_{\text{av}} \tau_{\text{res}}^2(\vec{k}) v^2(\vec{k}) dS}{\left( \int_{\text{FS}} \tau_{\text{res}}(\vec{k}) v(\vec{k}) dS \right)^2}. \quad (9)$$

In order to explain the systematic dependence of  $R_H^0$  on the valence of the 3d impurities (Fig. 5), the model proposed in I will be modified, because the Coulomb scattering part, being small, will be neglected. Using the three-group model of the Fermi surface of aluminum<sup>18-22</sup> and the above assumption for the nonresonant part of the relaxation time, Kesternich's formula of the low-field

$$R_H^0 = R_{\text{FE}} + A \left( \frac{(\cot^4 \eta_2^{++} - \cot^4 \eta_2^{--})_{\text{res}} + 2(\cot^2 \eta_2^{++} - \cot^2 \eta_2^{--})_{\text{res}}}{(1 + 2 \cot^2 \eta_2^+ + \cot^4 \eta_2^+)_{\text{res}}} \right), \quad (11)$$

where  $\eta_2^+$ ,  $\eta_2^-$ , and  $\eta_2^{++}$  are the phase shifts on the free-electron-like, strongly electronlike, and

Hall coefficient<sup>22</sup>  $R_H^0$  can be written in the form

$$R_H^0 = R_{\text{FE}} + A \left( \frac{(l_{\text{res}}^{++})^2 - (l_{\text{res}}^{--})^2}{(l_{\text{res}}^+)^2} \right). \quad (10)$$

Here  $R_{\text{FE}} = -3.47 \times 10^{-5} \text{ cm}^3/\text{As}$  is the free-electron value of the Hall coefficient,  $A = 6.5 \times 10^{-5} \text{ cm}^3/\text{As}$ ,  $(l_{\text{res}}^-)$ ,  $(l_{\text{res}}^{--})$ , and  $(l_{\text{res}}^{++})$  are the respective mean free paths due to the resonant scattering of the free-electron-like, strongly electronlike, and strongly holelike Fermi-surface regions of Al.

For

$$l_{\text{res}}^{-1} = [20v_F c / \pi \hbar N(\epsilon_F)] \sin^2 \eta_2^{\text{res}},$$

the expression (10) for the low-field Hall coefficient  $R_H^0$  may be written as

strongly holelike Fermi-surface regions. In the case where  $\eta_2^{++} = \eta_2^{--}$  the free-electron value  $R_{\text{FE}}$

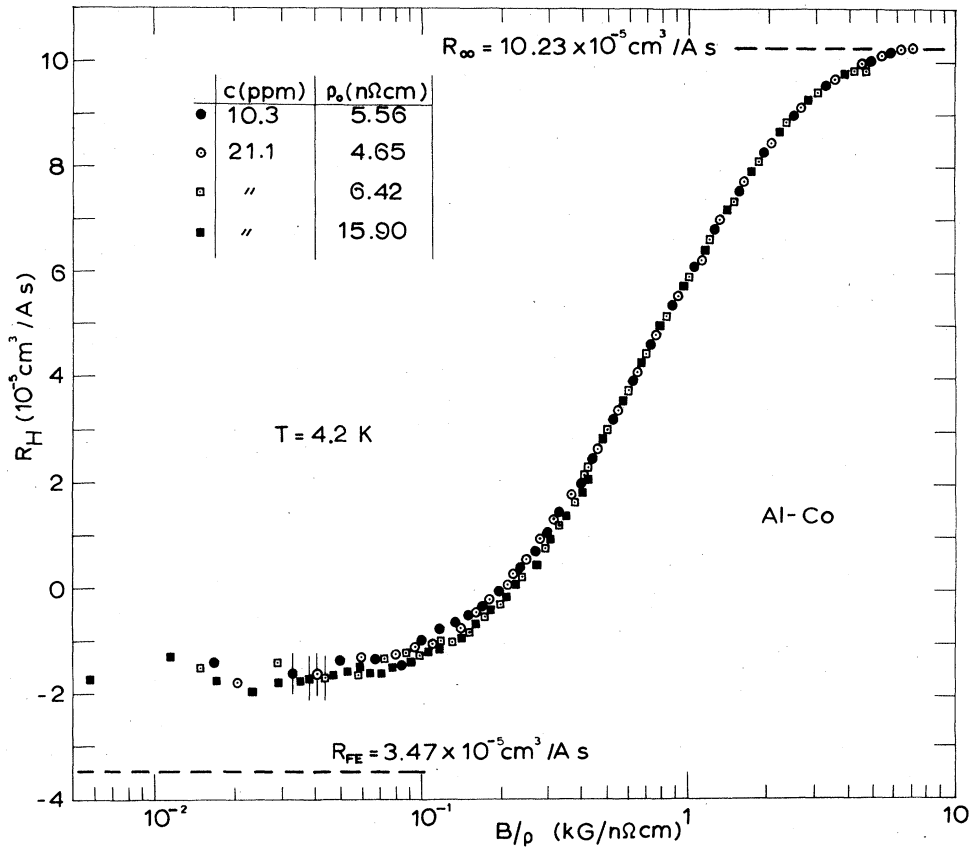


FIG. 4. Kohler plot of the Hall coefficient  $R_H$  as a function of  $B/\rho_0$  for the Al-Co alloys.

can be obtained. When  $\eta_2^{*+} < \eta_2^{-}$  the value of  $R_H^0$  is larger than  $R_{FE}$ , whereas for  $\eta_2^{*+} > \eta_2^{-}$   $R_H^0$  is smaller than  $R_{FE}$ .

The observed systematic dependence of the low-field Hall coefficient  $R_H^0$  of the dilute alloys of Al on the atomic number of solutes can be readily attributed to differences in the scattering probabilities of the VBS near the second- and third-zone Fermi surface edges. In the spirit of Friedel-Anderson,<sup>15,16</sup> when the atomic number of the solute increases from scandium to copper, the corresponding virtual state sinks into the Fermi sea of the aluminum conduction band. For chromium and manganese the VBS cross the Fermi level, where the resonant energies coincide with the level.

The experimentally determined low-field Hall coefficient  $R_H^0$  has the lowest values for the Al-Cr and Al-Mn alloys, and even tends to the free-electron value  $R_{FE}$  (Fig. 5). The assumption that this result is not highly accidental then implies that the phase shifts  $\eta_2^{*+}$  and  $\eta_2^{-}$  are almost equal. When the VBS associated with the Cr and Mn impurities cross the Fermi level of Al, the phase

shifts  $\eta_2^{*+}$  and  $\eta_2^{-}$  tend to  $\pi/2$ . This means that in this case the corresponding contributions from the highly curved Fermi-surface regions to  $R_H^0$  cancel.

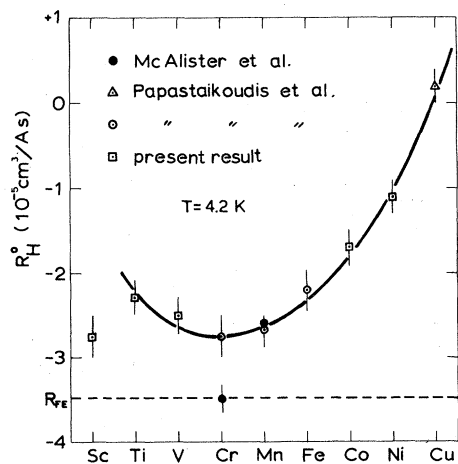


FIG. 5. The low-field Hall coefficient  $R_H^0$  of aluminum alloys plotted vs atomic number of the impurity.

On both sides of Cr and Mn impurities, namely, when the VBS moves far from the Fermi level of Al, the low-field Hall coefficient  $R_H^0$  increases and in the case of Cu impurity even changes sign and becomes positive. This means that the phase shifts on both sides of Cr and Mn must satisfy the condition  $\eta_2^{++} < \eta_2^{--}$ ; i.e., the phase shift  $\eta_2^{++}$  on the second zone will become smaller than the phase shift on the third zone, when the VBS moves far away from  $\epsilon_F$  of Al.

To relate the behavior of the phase shift  $\eta_2^{\text{res}}$  to the position of the virtual  $d$ -bound states relative to Fermi level, which occurs in the alloying of aluminum, one must consider the electron wave functions  $\psi_{\vec{k}}(\vec{r})$ . For  $\vec{k}$  states on a Brillouin-zone boundary (BZB) in the second zone of aluminum the  $\psi_{\vec{k}}(\vec{r})$  exhibits  $p$ -like character, while for  $\vec{k}$  states in the third zone the  $\psi_{\vec{k}}(\vec{r})$  is an admixture of  $s$  character. On the free-electron-like regions of the Fermi surface, the  $\psi_{\vec{k}}(\vec{r})$  represent a plane wave.

Thus, in the case of Al-Cr and Al-Mn alloys, the electrons at the holelike edges in the second zone and the electrons at the electronlike edges in the third zone will be scattered approximately with similar probability on Cr and Mn impurities.

When one now moves away from Cr and Mn, the  $3d$ -VBS is displaced from the Fermi level of Al, and then the VBS begins to scatter the electrons on the electronlike edges in the third zone at the cost of the electrons at the holelike edges in the second zone.

At the two ends of the  $3d$  transitional period, i.e., Ti and Cu, the scattering probability of the electrons on the electronlike edges in the third zone is strongest. Hence the two  $3d$  elements in aluminum cause the low-field Hall coefficient  $R_H^0$  values to be largest. The unexpected low  $R_H^0$  value for Al-Sc alloys does not agree with the VBS model. At the moment this deviation from the parabolic curve cannot be explained.

## V. CONCLUSIONS

The present measurements of the low-field Hall coefficient  $R_H^0$  of the Al-Sc, Al-Ti, Al-V, Al-Co, and Al-Ni alloys, together with previous measurements on Al-Cr, Al-Mn, and Al-Fe alloys, have shown that  $R_H^0$  depends systematically on the atomic  $d$  occupation number with an exception for the Al-Sc alloys. The  $R_H^0$  has a parabolic dependence on the valence of the impurity and reaches the lowest value at Cr. This dependence has been interpreted as due to the existence of the virtual bound state.

## ACKNOWLEDGMENTS

The authors are very grateful to Dr. B. Lengeler from Institut für Festkörperforschung, Kernforschungsanlage, Jülich, for the sample preparation and Dr. G. Papaioannou for careful reading of the manuscript.

<sup>1</sup>C. M. Hurd, *The Hall Effect in Metals and Alloys* (Plenum, New York 1972).

<sup>2</sup>M. Tsuji, *J. Phys. Soc. Jpn.* **13**, 979 (1958).

<sup>3</sup>K. Böning, *Phys. Kondens. Mater.* **11**, 177 (1970).

<sup>4</sup>C. Papastaikoudis, D. Papadimitropoulos, and E. Roco-fyllou, *Phys. Rev. B* **22**, 2670 (1980).

<sup>5</sup>G. Boato, M. Bugo, and C. Rizzuto, *Nuovo Cimento* **45**, 226 (1966).

<sup>6</sup>C. Papastaikoudis, E. Thanou, D. Tsamakis, and W. Tselfes, *J. Low Temp. Phys.* **34**, 429 (1979).

<sup>7</sup>E. Babic, R. Krsnik, B. Leontic, M. Ocko, Z. Vucic, and I. Zoric, *Solid State Commun.* **10**, 691 (1972).

<sup>8</sup>E. Babic, R. Krsnik, and M. Ocko, *J. Phys. F* **6**, 73 (1976).

<sup>9</sup>R. Aoki and T. Ohtsuka, *J. Phys. Soc. Jpn.* **23**, 955 (1967).

<sup>10</sup>R. Krsnik, E. Babic, and C. Rizzuto, *Solid State Commun.* **12**, 891 (1973).

<sup>11</sup>M. Ocko, E. Babic, R. Krsnik, E. Girt, and B. Leon-

tic, *J. Phys. F* **6**, 703 (1976).

<sup>12</sup>S. Fujikawa, M. Sugava, H. Takei, and K. Hinaro, *J. Less-Common Met.* **63**, 87 (1979).

<sup>13</sup>F. R. Fickett, *Cryogenics* **11**, 349 (1971).

<sup>14</sup>S. P. McAlister, C. M. Hurd, and L. R. Lupton, *J. Phys. F* **9**, 1849 (1979).

<sup>15</sup>J. Friedel, *Nuovo Cimento Suppl.* **7**, 287 (1958).

<sup>16</sup>P. W. Anderson, *Phys. Rev.* **124**, 41 (1961).

<sup>17</sup>A. P. Klein and A. J. Heeger, *Phys. Rev.* **144**, 458 (1966).

<sup>18</sup>R. S. Sorbello, *J. Phys. F* **4**, 1665 (1974).

<sup>19</sup>K. Böning, K. Pfänder, P. Rosner, and M. Schlüter, *J. Phys. F* **5**, 1176 (1975).

<sup>20</sup>W. Kesternich, H. Ullmaier, and W. Schilling, *J. Phys. F* **6**, 1867 (1976).

<sup>21</sup>K. Pfänder, K. Böning, and W. Brening, *Z. Phys. B* **32**, 287 (1979).

<sup>22</sup>W. Kesternich, *Phys. Rev. B* **13**, 4227 (1976).